

# SOUND FIELD REPRODUCTION WITH EXTERIOR CANCELLATION USING ANALYTICAL WEIGHTING OF HARMONIC COEFFICIENTS

Natsuki Ueno<sup>1</sup>, Shoichi Koyama<sup>1,2</sup>, Hiroshi Saruwatari<sup>1</sup>

<sup>1</sup>The University of Tokyo, Graduate School of Information Science and Technology,  
7-3-1 Hongo, Bunkyo-ku, Tokyo 113-8656, Japan

<sup>2</sup>Institut Langevin, ESPCI, Paris Diderot University, CNRS UMR 7587,  
1 rue Jessieu, Paris 75005, France

## ABSTRACT

A method for sound field reproduction with the suppression of exterior radiation is proposed, which makes it possible to synthesize a desired sound field in a reverberant environment without prior knowledge of the transfer functions of the multiple loudspeakers. The objective function used to achieve this is formulated as the weighted sum of the interior reproduction error and exterior radiation power. The optimal driving signals are derived by harmonic expansion of both the interior and exterior sound fields. In contrast to the empirical coefficient truncation in the state of the art, in the proposed method, an optimal weighting of the harmonic coefficients is derived analytically. Numerical simulation results indicated that high interior reproduction accuracy and exterior power suppression can be achieved by the proposed method compared with the mode-matching method using harmonic-order truncation owing to the optimal weighting.

**Index Terms**— sound field reproduction, exterior cancellation, circular harmonics, loudspeaker array.

## 1. INTRODUCTION

Sound field reproduction aims at the physical synthesis of a desired sound field over a target area using multiple loudspeakers. Analytical approaches to sound field reproduction [1–6] (e.g., wave field synthesis and higher-order ambisonics), whose principal theory is based on physical acoustics, have been investigated, particularly in the last decade. In these methods, transfer functions of the loudspeakers are typically assumed as analytical directivity functions, i.e., linear combinations of multipoles or even monopoles [7]. This assumption obviously limits their feasibility in a reverberant environment.

One possible approach to overcome the reverberation problem is to measure the transfer functions inside the target area by using multiple microphones [8, 9]. Since it is necessary to measure the transfer functions between large numbers of microphones and loudspeakers, this approach can be practically difficult. Moreover, the transfer functions can vary with changes in the room environment.

A prospective alternative approach is to suppress exterior radiation outside the loudspeakers (i.e., *exterior cancellation*) as well as to reproduce the desired sound field inside the target area. Poletti and Abhayapala [10] proposed a method based on the Kirchhoff–Helmholtz equation [11], whose basic idea is that the sound field can be reproduced without exterior radiation by using a continuous distribution of monopoles and dipoles. Since it is difficult to continuously place monopoles and dipoles and to individually control them in practice, they are generally replaced by a double-layer array of

loudspeakers [12, 13]. It was also shown that exterior radiation can be reduced to some extent by using a single-layer array of loudspeakers with fixed directivity [14]. A more flexible and comprehensive approach is the *mode-matching method*, which aims to control harmonic coefficients of a sound field. The mode-matching method was applied to an array of higher-order loudspeakers to control the more complex directivity pattern of each array element and to jointly control the interior and exterior sound fields by Poletti et al. [15]. It is worth noting that the same formulation can also be applied to other array geometries such as a double-layer array. However, it is necessary in the mode-matching method to truncate harmonic coefficients in an empirical manner, which strongly affects its reproduction and cancellation performances.

We propose a method for sound field reproduction with exterior cancellation based on an analytical weighting of harmonic coefficients. As in the mode-matching method, our proposed method is formulated so as to be applicable to any type of array geometry and directivity of loudspeakers. An objective function to be minimized is formulated as a weighted sum of the reproduction error of the synthesized interior sound field and the exterior power radiation outside the loudspeakers. The optimal driving signals are derived by harmonic expansion of the interior and exterior sound fields, incorporating the analytically derived weighting of the harmonic coefficients. The use of the optimally weighted harmonic coefficients without truncation errors enables high interior reproduction accuracy and exterior suppression. Numerical experiments are performed to demonstrate that the proposed method outperforms the current mode-matching method.

## 2. PRELIMINARIES

First, we introduce several basic theories and definitions for the harmonic representation of a sound field as preliminaries. For simplicity, a two-dimensional (2D) sound field is considered in this paper; however, the proposed method can be extended to the three-dimensional (3D) case with several modifications.

Let  $\Omega$  be a circular area with center  $\mathbf{r}_0$ . The interior and exterior sound fields of  $\Omega$  are expanded around  $\mathbf{r}_0$  using circular harmonics as [11]

$$u(\mathbf{r}, \omega) = \sum_{\mu=-\infty}^{\infty} \hat{u}_{\mu}^{\text{int}}(\mathbf{r}_0, \omega) \varphi_{\mu}(\mathbf{r} - \mathbf{r}_0, \omega), \quad \mathbf{r} \in \Omega \quad (1)$$

and

$$u(\mathbf{r}, \omega) = \sum_{\mu=-\infty}^{\infty} \hat{u}_{\mu}^{\text{ext}}(\mathbf{r}_0, \omega) \psi_{\mu}(\mathbf{r} - \mathbf{r}_0, \omega), \quad \mathbf{r} \notin \Omega, \quad (2)$$

respectively. Here,  $u(\mathbf{r}, \omega)$  is the sound pressure of temporal frequency  $\omega$  at position  $\mathbf{r}$ , and  $\hat{u}_\mu^{\text{int}}(\mathbf{r}_0, \omega)$  and  $\hat{u}_\mu^{\text{ext}}(\mathbf{r}_0, \omega)$  are the interior and exterior harmonic coefficients, respectively. The interior and exterior basis functions  $\varphi_\mu(\mathbf{r}, \omega)$  and  $\psi_\mu(\mathbf{r}, \omega)$  are respectively defined in polar coordinates  $\mathbf{r} = (r, \phi)$  as

$$\varphi_\mu(\mathbf{r} - \mathbf{r}_0, \omega) = J_\mu(kr)\exp(j\mu\phi) \quad (3)$$

$$\psi_\mu(\mathbf{r} - \mathbf{r}_0, \omega) = H_\mu(kr)\exp(j\mu\phi), \quad (4)$$

where  $k = \omega/c$  is the wave number with sound velocity  $c$ ,  $J_\mu(\cdot)$  is the  $\mu$ th-order Bessel function of the first kind, and  $H_\mu(\cdot)$  is the  $\mu$ th-order Hankel function.

The coefficients  $\hat{u}_\mu^{\text{int}}(\mathbf{r}_0, \omega)$  and  $\hat{u}_\mu^{\text{ext}}(\mathbf{r}_0, \omega)$  have the following relations:

$$\hat{u}_\mu^{\text{ext}}(\mathbf{r}_0, \omega) = \sum_{\mu'=-\infty}^{\infty} T_{\mu, \mu'}(\mathbf{r}_0 - \mathbf{r}'_0, \omega) \hat{u}_{\mu'}^{\text{ext}}(\mathbf{r}'_0, \omega) \quad (5)$$

$$\hat{u}_\mu^{\text{int}}(\mathbf{r}_0, \omega) = \sum_{\mu'=-\infty}^{\infty} S_{\mu, \mu'}(\mathbf{r}_0 - \mathbf{r}'_0, \omega) \hat{u}_{\mu'}^{\text{ext}}(\mathbf{r}'_0, \omega), \quad (6)$$

where  $T_{\mu, \mu'}(\mathbf{r}, \omega)$  and  $S_{\mu, \mu'}(\mathbf{r}, \omega)$  are the translation operators defined as [16]

$$T_{\mu, \mu'}(\mathbf{r}, \omega) = (-1)^{\mu-\mu'} J_{\mu-\mu'}(kr)\exp(-j(\mu-\mu')\phi) \quad (7)$$

$$S_{\mu, \mu'}(\mathbf{r}, \omega) = (-1)^{\mu-\mu'} H_{\mu-\mu'}(kr)\exp(-j(\mu-\mu')\phi). \quad (8)$$

As shown in [16], the operator  $T_{\mu, \mu'}(\mathbf{r}, \omega)$  satisfies the following equations:

$$T_{\mu, \mu'}(-\mathbf{r}, \omega) = T_{\mu', \mu}(\mathbf{r}, \omega)^* \quad (9)$$

$$T_{\mu, \mu'}(\mathbf{r} + \mathbf{r}', \omega) = \sum_{\mu''=-\infty}^{\infty} T_{\mu, \mu''}(\mathbf{r}, \omega) T_{\mu'', \mu'}(\mathbf{r}', \omega). \quad (10)$$

Hereafter,  $\omega$  is omitted for notational simplicity.

### 3. OBJECTIVE FUNCTION FOR JOINT INTERIOR REPRODUCTION AND EXTERIOR CANCELLATION

Now, we formulate the objective function for jointly achieving the reproduction of a desired sound field and suppression of the exterior radiation. Suppose that  $L$  secondary sources (i.e., loudspeakers) are located at  $\mathbf{r}_1, \dots, \mathbf{r}_L$  with an arbitrary array geometry. All the secondary sources are assumed to be inside a circular region  $\Omega_S$  with center  $\mathbf{r}_S$ . The driving signal and transfer function of the  $l$ th secondary source are denoted by  $d_l$  and  $g_l(\mathbf{r})$ , respectively. The sound field synthesized by the  $L$  secondary sources is represented as

$$u_{\text{syn}}(\mathbf{r}) = \sum_{l=1}^L d_l g_l(\mathbf{r}). \quad (11)$$

In the free field, the transfer function  $g_l(\mathbf{r})$  can be expanded around  $\mathbf{r}_l$  by using  $\psi_\mu(\mathbf{r} - \mathbf{r}_l)$  as

$$g_l(\mathbf{r}) = \sum_{\mu=-\infty}^{\infty} \beta_{l, \mu} \psi_\mu(\mathbf{r} - \mathbf{r}_l), \quad (12)$$

where the coefficient  $\beta_{l, \mu}$  corresponds to the directivity of the  $l$ th secondary source. We assume that  $\beta_{l, \mu}$  is obtained by modeling or measuring the directivity.

Our objective is twofold. One is to synthesize a desired sound field inside a given reproduction area  $\Omega_{\text{syn}}$ . This can be achieved by

solving the following optimization problem:

$$\text{minimize}_{\mathbf{d} \in \mathbb{C}^L} \mathcal{J}_{\text{int}}(\mathbf{d}) = \int_{\Omega_{\text{syn}}} w(\mathbf{r}) |u_{\text{syn}}(\mathbf{r}) - u_{\text{des}}(\mathbf{r})|^2 d\mathbf{r}, \quad (13)$$

where  $\mathbf{d} = [d_1, \dots, d_L]^T$  is the vector of the driving signals,  $u_{\text{des}}(\mathbf{r})$  is the desired sound pressure, and  $w(\mathbf{r})$  is a spatial weighting function. The other is to suppress exterior acoustic radiation from the secondary sources. This can be achieved by solving the following optimization problem:

$$\text{minimize}_{\mathbf{d} \in \mathbb{C}^L} \mathcal{J}_{\text{ext}}(\mathbf{d}) = \int_{\partial\Omega_S} I_{\text{ext}}(\mathbf{r}) d\mathbf{r}, \quad (14)$$

where  $\partial\Omega_S$  is the boundary of  $\Omega_S$  and  $I_{\text{ext}}(\mathbf{r})$  is the acoustic intensity in the outward normal direction defined as [11]

$$I_{\text{ext}}(\mathbf{r}) = \frac{1}{2} \text{Re} \left[ u_{\text{syn}}(\mathbf{r}) \frac{j}{\rho c k} \frac{\partial}{\partial \mathbf{n}} u_{\text{syn}}(\mathbf{r})^* \right]. \quad (15)$$

Here,  $\rho$  is the density of air,  $\text{Re}[\cdot]$  denotes the real part of the complex number, and  $\partial/\partial \mathbf{n}$  denotes the normal derivative. The right side of (14) represents the total acoustic power radiated by the  $L$  secondary sources. To jointly achieve the above two objectives (13) and (14), we consider the following optimization problem:

$$\text{minimize}_{\mathbf{d} \in \mathbb{C}^L} \mathcal{J}(\mathbf{d}) = \mathcal{J}_{\text{int}}(\mathbf{d}) + \gamma \mathcal{J}_{\text{ext}}(\mathbf{d}), \quad (16)$$

where  $\gamma \in [0, \infty)$  is a constant parameter used to balance the two objective functions.

### 4. DERIVATION OF OPTIMAL DRIVING SIGNALS

We here derive the optimal driving signals minimizing  $\mathcal{J}(\mathbf{d})$  on the basis of the harmonic analysis introduced in Sect. 2. First,  $\mathcal{J}_{\text{int}}(\mathbf{d})$  is rewritten by substituting (11) into (13) as

$$\mathcal{J}_{\text{int}}(\mathbf{d}) = \mathbf{d}^H \mathbf{A}_{\text{int}} \mathbf{d} - \mathbf{d}^H \mathbf{b}_{\text{int}} - \mathbf{b}_{\text{int}}^H \mathbf{d} + c_{\text{int}}, \quad (17)$$

where  $\mathbf{A}_{\text{int}} \in \mathbb{C}^{L \times L}$ ,  $\mathbf{b}_{\text{int}} \in \mathbb{C}^L$ , and  $c_{\text{int}} \in \mathbb{R}$  are given by

$$(\mathbf{A}_{\text{int}})_{l_1, l_2} = \int_{\Omega_{\text{syn}}} w(\mathbf{r}) g_{l_1}(\mathbf{r})^* g_{l_2}(\mathbf{r}) d\mathbf{r} \quad (18)$$

$$(\mathbf{b}_{\text{int}})_l = \int_{\Omega_{\text{syn}}} w(\mathbf{r}) g_l(\mathbf{r})^* u_{\text{des}}(\mathbf{r}) d\mathbf{r} \quad (19)$$

$$c_{\text{int}} = \int_{\Omega_{\text{syn}}} w(\mathbf{r}) |u_{\text{des}}(\mathbf{r})|^2 d\mathbf{r}. \quad (20)$$

Here,  $(\cdot)_{l_1, l_2}$  denotes the  $(l_1, l_2)$ th element of the matrix and  $(\cdot)_l$  denotes the  $l$ th element of the vector. Although (18), (19), and (20) include a domain integral, they can be efficiently calculated without a numerical integral by expanding the sound field inside  $\Omega_{\text{syn}}$  for several  $w(\mathbf{r})$  [17, 18]. In this paper, we focus on the case where  $\Omega_{\text{syn}}$  is a single circular area with center  $\mathbf{r}_{\text{syn}}$  and radius  $R_{\text{syn}}$  and  $w(\mathbf{r})$  is the uniform distribution on  $\Omega_{\text{syn}}$  [17]. The transfer functions and the desired sound field are expanded around  $\mathbf{r}_{\text{syn}}$  as

$$g_l(\mathbf{r}) = \sum_{\mu=-\infty}^{\infty} g_{l, \mu}^{\text{int}}(\mathbf{r}_{\text{syn}}) \varphi_\mu(\mathbf{r} - \mathbf{r}_{\text{syn}}), \quad \mathbf{r} \in \Omega_{\text{syn}} \quad (21)$$

$$u_{\text{des}}(\mathbf{r}) = \sum_{\mu=-\infty}^{\infty} \hat{u}_{\text{des}, \mu}^{\text{int}}(\mathbf{r}_{\text{syn}}) \varphi_\mu(\mathbf{r} - \mathbf{r}_{\text{syn}}), \quad \mathbf{r} \in \Omega_{\text{syn}}. \quad (22)$$

The interior harmonic coefficient of  $g_l(\mathbf{r})$  is obtained from (6) and (12) as

$$\hat{g}_{l,\mu}^{\text{int}}(\mathbf{r}_{\text{syn}}) = \sum_{\mu'=-\infty}^{\infty} S_{\mu,\mu'}(\mathbf{r}_{\text{syn}} - \mathbf{r}_l) \beta_{l,\mu'}. \quad (23)$$

By substituting (21) and (22) into (18) and (19), we obtain

$$(\mathbf{A}_{\text{int}})_{l_1,l_2} = \sum_{\mu=-\infty}^{\infty} \hat{w}_{\mu} \hat{g}_{l_1,\mu}^{\text{int}}(\mathbf{r}_{\text{syn}})^* \hat{g}_{l_2,\mu}^{\text{int}}(\mathbf{r}_{\text{syn}}) \quad (24)$$

$$(\mathbf{b}_{\text{int}})_l = \sum_{\mu=-\infty}^{\infty} \hat{w}_{\mu} \hat{g}_{l,\mu}^{\text{int}}(\mathbf{r}_{\text{syn}})^* \hat{u}_{\text{des},\mu}^{\text{int}}(\mathbf{r}_{\text{syn}}) \quad (25)$$

with

$$\begin{aligned} \hat{w}_{\mu} &= \int_{\Omega_{\text{syn}}} w(\mathbf{r}) |\varphi_{\mu}(\mathbf{r})|^2 d\mathbf{r} \\ &= J_{\mu}(kR_{\text{syn}})^2 - J_{\mu-1}(kR_{\text{syn}})J_{\mu+1}(kR_{\text{syn}}). \end{aligned} \quad (26)$$

Equations (24) and (25) can be calculated by truncating the summation at a sufficiently large order because  $\hat{w}_{\mu}$  sufficiently decays for large  $\mu$ . The detailed derivation of the above equations is given in [17].

Next,  $\mathcal{J}_{\text{ext}}(\mathbf{d})$  is simplified in a similar manner as described in [11] for the 3D case as

$$\mathcal{J}_{\text{ext}}(\mathbf{d}) = \frac{2}{\rho c k} \sum_{\mu=-\infty}^{\infty} |\hat{u}_{\text{syn},\mu}^{\text{ext}}(\mathbf{r}_{\text{S}})|^2. \quad (27)$$

The exterior harmonic coefficient  $\hat{u}_{\text{syn},\mu}^{\text{ext}}(\mathbf{r}_{\text{S}})$  is represented as

$$\hat{u}_{\text{syn},\mu}^{\text{ext}}(\mathbf{r}_{\text{S}}) = \sum_{l=1}^L d_l \hat{g}_{l,\mu}^{\text{ext}}(\mathbf{r}_{\text{S}}). \quad (28)$$

From (5), (27), and (28), we obtain

$$\mathcal{J}_{\text{ext}}(\mathbf{d}) = \mathbf{d}^H \mathbf{A}_{\text{ext}} \mathbf{d}, \quad (29)$$

where  $\mathbf{A}_{\text{ext}} \in \mathbb{C}^{L \times L}$  is given by

$$\begin{aligned} (\mathbf{A}_{\text{ext}})_{l_1,l_2} &= \frac{2}{\rho c k} \sum_{\mu=-\infty}^{\infty} \hat{g}_{l_1,\mu}^{\text{ext}}(\mathbf{r}_{\text{S}})^* \hat{g}_{l_2,\mu}^{\text{ext}}(\mathbf{r}_{\text{S}}) \\ &= \frac{2}{\rho c k} \sum_{\mu_1=-\infty}^{\infty} \sum_{\mu_2=-\infty}^{\infty} \beta_{l_1,\mu_1}^* \beta_{l_2,\mu_2} \\ &\quad \cdot \sum_{\mu=-\infty}^{\infty} T_{\mu,\mu_1}(\mathbf{r}_{\text{S}} - \mathbf{r}_{l_1})^* T_{\mu,\mu_2}(\mathbf{r}_{\text{S}} - \mathbf{r}_{l_2}) \\ &= \frac{2}{\rho c k} \sum_{\mu_1=-\infty}^{\infty} \sum_{\mu_2=-\infty}^{\infty} \beta_{l_1,\mu_1}^* \beta_{l_2,\mu_2} T_{\mu_1,\mu_2}(\mathbf{r}_{l_1} - \mathbf{r}_{l_2}). \end{aligned} \quad (30)$$

The last line of (30) is derived by applying (9) and (10) to the second line. This equation indicates that  $\mathbf{A}_{\text{ext}}$  is independent of the position and size of  $\Omega_{\text{S}}$ . Furthermore, when the directivity of the secondary sources is represented by a finite order  $N$  (i.e.,  $\beta_{l,\mu} = 0$  for  $|\mu| > N$ ), the summations in (30) consist of finite elements and can be accurately calculated without truncation errors.

Finally,  $\mathcal{J}(\mathbf{d})$  is rewritten as

$$\mathcal{J}(\mathbf{d}) = \mathbf{d}^H (\mathbf{A}_{\text{int}} + \gamma \mathbf{A}_{\text{ext}}) \mathbf{d} - \mathbf{d}^H \mathbf{b}_{\text{int}} - \mathbf{b}_{\text{int}}^H \mathbf{d} + c_{\text{int}}. \quad (31)$$

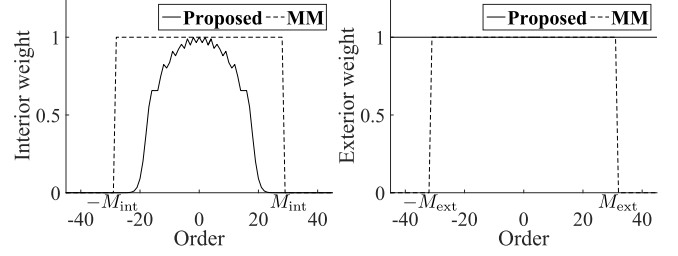


**Fig. 1:** Interior and exterior weights in proposed method (**Proposed**) and mode-matching method (**MM**).

Since (31) is a quadratic function of  $\mathbf{d}$ , the optimal driving signals  $\hat{\mathbf{d}}$  are given by

$$\hat{\mathbf{d}} = (\mathbf{A}_{\text{int}} + \gamma \mathbf{A}_{\text{ext}} + \lambda \mathbf{I}_L)^{-1} \mathbf{b}_{\text{int}}, \quad (32)$$

where  $\mathbf{I}_L$  is the  $L \times L$  identity matrix and  $\lambda \in [0, \infty)$  is a regularization parameter.

## 5. COMPARISON WITH MODE-MATCHING METHOD

We here discuss the difference between the proposed method and the mode-matching method [15]. In the mode-matching method, the driving signals are obtained by solving the following mode-matching equations:

$$\sum_{l=1}^L d_l \hat{g}_{l,\mu}^{\text{int}}(\mathbf{r}_{\text{syn}}) = \hat{u}_{\text{des},\mu}^{\text{int}}(\mathbf{r}_{\text{syn}}), \quad \mu \in \{-M_{\text{int}}, \dots, M_{\text{int}}\} \quad (33)$$

$$\sum_{l=1}^L d_l \hat{g}_{l,\mu}^{\text{ext}}(\mathbf{r}_{\text{S}}) = 0, \quad \mu \in \{-M_{\text{ext}}, \dots, M_{\text{ext}}\}, \quad (34)$$

where  $M_{\text{int}}$  and  $M_{\text{ext}}$  are truncation orders. The solution of (33) and (34) is

$$\mathbf{d} = (\bar{\mathbf{A}}_{\text{int}} + \bar{\mathbf{A}}_{\text{ext}} + \lambda \mathbf{I}_L)^{-1} \bar{\mathbf{b}}_{\text{int}} \quad (35)$$

with

$$(\bar{\mathbf{A}}_{\text{int}})_{l_1,l_2} = \sum_{\mu=-M_{\text{int}}}^{M_{\text{int}}} \hat{g}_{l_1,\mu}^{\text{int}}(\mathbf{r}_{\text{syn}})^* \hat{g}_{l_2,\mu}^{\text{int}}(\mathbf{r}_{\text{syn}}) \quad (36)$$

$$(\bar{\mathbf{b}}_{\text{int}})_l = \sum_{\mu=-M_{\text{int}}}^{M_{\text{int}}} \hat{g}_{l,\mu}^{\text{int}}(\mathbf{r}_{\text{syn}})^* \hat{u}_{\text{des},\mu}^{\text{int}}(\mathbf{r}_{\text{syn}}) \quad (37)$$

$$(\bar{\mathbf{A}}_{\text{ext}})_{l_1,l_2} = \sum_{\mu=-M_{\text{ext}}}^{M_{\text{ext}}} \hat{g}_{l_1,\mu}^{\text{ext}}(\mathbf{r}_{\text{S}})^* \hat{g}_{l_2,\mu}^{\text{ext}}(\mathbf{r}_{\text{S}}). \quad (38)$$

By comparing (24), (25), and the first line of (30) with (36), (37), and (38), respectively, we can see that the difference between these two methods is in the weighting of the interior and exterior harmonic coefficients. Figure 1 shows an example of the weights in the proposed method and the mode-matching method for  $kR_{\text{syn}} = 20$  rad. Here, the weights are scaled so that the zeroth-order values correspond to 1. In the mode-matching method, appropriate truncation orders  $M_{\text{int}}$  and  $M_{\text{ext}}$  have to be determined in an empirical manner. In the proposed method, on the other hand, the interior and exterior harmonic coefficients are optimally weighted, where the weights are derived analytically by (26) and (30). Note that the infinite-order exterior harmonic coefficients are uniformly weighted by (30).

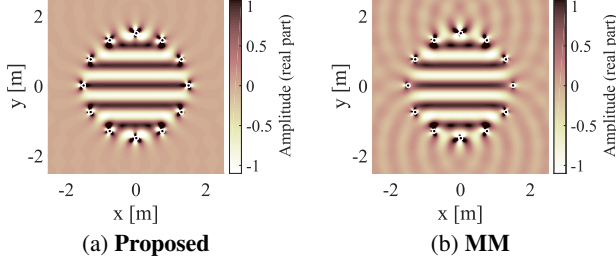


Fig. 2: Reproduced sound pressure distributions at 600 Hz.

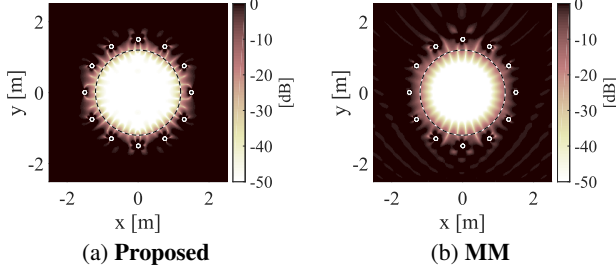


Fig. 3: Normalized error distributions at 600 Hz.

## 6. NUMERICAL SIMULATIONS

Numerical simulations were conducted to evaluate the proposed method using a circular higher-order loudspeaker array in comparison with the mode-matching method [15]. The circular array consists of 12 ideal third-order loudspeakers. The proposed and mode-matching methods are denoted as **Proposed** and **MM**, respectively. In Cartesian coordinates  $\mathbf{r} = (x, y)$ , the center and radius of the circular array were set to  $(0.0, 0.0)$  m and 1.5 m, respectively. Each third-order loudspeaker was assumed to be seven individual multipoles (from -3rd to 3rd order), and the amplitude of the  $\mu$ th-order multipole was set to  $1/kR_{\text{hol}}H'_\mu(kR_{\text{hol}})$  with  $R_{\text{hol}} = 0.2$  m as described in [15]. The sound speed was set to 340.29 m/s. The desired sound field was a plane wave propagating in the  $y$  direction, i.e.,  $u_{\text{des}}(\mathbf{r}) = \exp(jky)$ .

In **Proposed**, the reproduction area  $\Omega_{\text{syn}}$  was set as a single circular area with center  $(0.0, 0.0)$  m and radius 1.2 m, and (24) and (25) were truncated at  $\mu = \pm[5kR_{\text{syn}}]$ . In **MM**, the truncation orders  $M_{\text{int}}$  and  $M_{\text{ext}}$  were determined as described in [15] with a mode order regulation factor of 0.75. For fair comparison between **Proposed** and **MM**,  $\mathbf{A}_{\text{int}}$  and  $\mathbf{b}_{\text{int}}$  were scaled by  $1/\hat{v}_0$  and  $\gamma$  was set as  $\rho ck/2$  in **Proposed** as in Fig. 1. The regularization parameter  $\lambda$  was set as  $1.0 \times 10^{-3}$  in both methods.

To evaluate the reproduction accuracy and exterior cancellation performances, we define the signal-to-distortion ratio (SDR) and suppression-power ratio (SPR) as

$$\text{SDR}(\omega) = 10 \log_{10} \frac{\int_{\Omega_{\text{syn}}} |u_{\text{des}}(\mathbf{r}, \omega)|^2 d\mathbf{r}}{\int_{\Omega_{\text{syn}}} |u_{\text{syn}}(\mathbf{r}, \omega) - u_{\text{des}}(\mathbf{r}, \omega)|^2 d\mathbf{r}} \quad (39)$$

$$\text{SPR}(\omega) = 10 \log_{10} \frac{\int_{\Omega_{\text{ext}}} |u_{\text{des}}(\mathbf{r}, \omega)|^2 d\mathbf{r}}{\int_{\Omega_{\text{ext}}} |u_{\text{syn}}(\mathbf{r}, \omega)|^2 d\mathbf{r}}, \quad (40)$$

where  $\Omega_{\text{ext}}$  was set as the area bounded by two circles of radii 2.0 and 2.5 m. Here,  $u_{\text{des}}(\mathbf{r})$  in (39) and (40) is the original desired sound field, i.e., the plane-wave field. SDRs and SPRs were calculated from 50 Hz to 1000 Hz at intervals of 50 Hz.

Figure 2 shows the reproduced pressure distribution at 600 Hz. The normalized error and power distributions,  $10 \log_{10} |u_{\text{syn}}(\mathbf{r}) -$

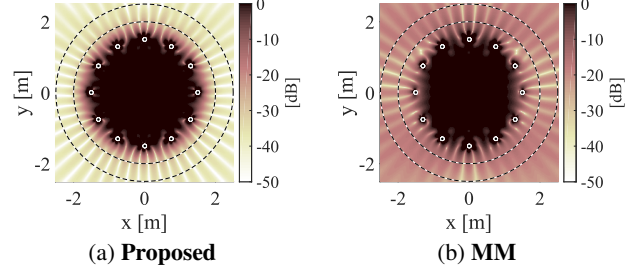


Fig. 4: Normalized power distributions at 600 Hz.

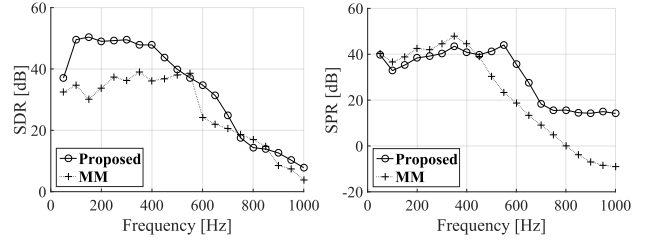


Fig. 5: SDR and SPR plotted against frequency.

$|u_{\text{syn}}(\mathbf{r})|^2/|u_{\text{des}}(\mathbf{r})|^2$  and  $10 \log_{10} |u_{\text{syn}}(\mathbf{r})|^2/|u_{\text{des}}(\mathbf{r})|^2$ , are also shown in Figs. 3 and 4, respectively, where  $u_{\text{des}}(\mathbf{r})$  is the plane-wave field in the entire region. The black dots represent the loudspeaker positions, and the dashed lines in Figs. 3 and 4 represent  $\Omega_{\text{syn}}$  and  $\Omega_{\text{ext}}$ , respectively. The SDRs of **Proposed** and **MM** were 34.46 and 24.23 dB, and their SPRs were 35.27 and 18.74 dB, respectively. The interior reproduction accuracy of **Proposed** was higher than that of **MM**, especially around the boundary of  $\Omega_{\text{syn}}$  (see Fig. 3). Furthermore, **Proposed** achieved high exterior radiation suppression, whereas undesired exterior radiation can be seen in **MM** (see Fig. 4). The principal cause of the performance degradation of **MM** in these results is the truncation of the harmonic coefficients at  $M_{\text{int}}$  and  $M_{\text{ext}}$ .

The SDR and SPR are plotted against the frequency in Fig. 5. At most frequencies, **Proposed** achieved a higher SDR than **MM**. The SPRs of both methods were comparable below 500 Hz; however, the SPR for **Proposed** above 500 Hz was much higher than that for **MM**, which is due to the optimal weighting of the harmonic coefficients.

## 7. CONCLUSION

We proposed a method for sound field reproduction with the suppression of exterior radiation. By minimizing an objective function consisting of the interior reproduction error and exterior radiation power, the optimal driving signals are derived on the basis of circular harmonic expansion of the interior and exterior sound fields. The advantage of the proposed method lies in the analytically derived weighting of the harmonic coefficients, whereas empirical truncation is required in the mode-matching method. The optimal weighting enables high reproduction accuracy and exterior power suppression compared with the current mode-matching method, which was validated by numerical experiments in 2D sound fields. Experimental validation in a practical 3D space will be a future work.

## 8. ACKNOWLEDGEMENTS

This work was supported by JSPS KAKENHI Grant Numbers JP15H05312 and JP16H01735 and SECOM Science and Technology Foundation.

## 9. REFERENCES

- [1] A. J. Berkhout, D. de Vries, and P. Vogel, "Acoustic control by wave field synthesis," *J. Acoust. Soc. Am.*, vol. 93, no. 5, pp. 2764–2778, 1993.
- [2] S. Spors, R. Rabenstein, and J. Ahrens, "The theory of wave field synthesis revisited," in *Proc. 124th AES Conv.*, Amsterdam, Oct. 2008.
- [3] J. Daniel, "Spatial sound encoding including near field effect: Introducing distance coding filters and a viable, new ambisonics format," in *Proc. 23rd AES Int. Conf.*, Copenhagen, May 2003.
- [4] M. A. Poletti, "Three-dimensional surround sound systems based on spherical harmonics," *J. Audio Eng. Soc.*, vol. 53, no. 11, pp. 1004–1025, 2005.
- [5] S. Koyama, K. Furuya, Y. Hiwasaki, and Y. Haneda, "Analytical approach to wave field reconstruction filtering in spatio-temporal frequency domain," *IEEE Trans. Audio, Speech, Lang. Process.*, vol. 21, no. 4, pp. 685–696, 2013.
- [6] S. Koyama, K. Furuya, Y. Hiwasaki, Y. Haneda, and Y. Suzuki, "Wave field reconstruction filtering in cylindrical harmonic domain for with-height recording and reproduction," *IEEE/ACM Trans. Audio, Speech, Lang. Process.*, vol. 22, no. 10, pp. 1546–1557, 2014.
- [7] S. Koyama, K. Furuya, Y. Hiwasaki, and Y. Haneda, "Sound field reproduction method in spatio-temporal frequency domain considering directivity of loudspeakers," in *Proc. 132nd AES Conv.*, Budapest, Apr. 2012.
- [8] T. Betlehem and T. D. Abhayapala, "Theory and design of sound field reproduction in reverberant rooms," *J. Acoust. Soc. Am.*, vol. 117, no. 4, pp. 2100–2111, 2005.
- [9] W. Jin and W. B. Kleijn, "Multizone soundfield reproduction in reverberant rooms using compressed sensing techniques," in *IEEE Int. Conf. Acoust., Speech, Signal Process. (ICASSP)*, May 2014, pp. 4728–4732.
- [10] M. A. Poletti and T. D. Abhayapala, "Interior and exterior sound field control using general two-dimensional first-order sources," *J. Acoust. Soc. Am.*, vol. 129, no. 1, pp. 234–244, 2011.
- [11] E. G. Williams, *Fourier Acoustics: Sound Radiation and Nearfield Acoustical Holography*, Academic Press, London, 1999.
- [12] J.-H. Chang and F. Jacobsen, "Sound field control with a circular double-layer array of loudspeakers," *J. Acoust. Soc. Am.*, vol. 131, no. 6, pp. 4518–4525, 2012.
- [13] T. Okamoto, "Analytical approach to 2.5D sound field control using a circular double-layer array of fixed-directivity loudspeakers," in *Proc. IEEE Int. Conf. Acoust., Speech, Signal Process. (ICASSP)*, Mar. 2017, pp. 91–95.
- [14] M. A. Poletti, F. M. Fazi, and P. A. Nelson, "Sound-field reproduction systems using fixed-directivity loudspeakers," *J. Acoust. Soc. Am.*, vol. 127, no. 6, pp. 3590–3601, 2010.
- [15] M. A. Poletti, T. D. Abhayapala, and P. Samarasinghe, "Interior and exterior sound field control using two dimensional higher-order variable-directivity sources," *The Journal of the Acoustical Society of America*, vol. 131, no. 5, pp. 3814–3823, 2012.
- [16] P. A. Martin, *Multiple Scattering: Interaction of Time-Harmonic Waves with N Obstacles*, Cambridge University Press, New York, 2006.
- [17] N. Ueno, S. Koyama, and H. Saruwatari, "Listening-area-informed sound field reproduction based on circular harmonic expansion," in *Proc. IEEE Int. Conf. Acoust., Speech, Signal Process. (ICASSP)*, New Orleans, Mar. 2017, pp. 111–115.
- [18] N. Ueno, S. Koyama, and H. Saruwatari, "Listening-area-informed sound field reproduction with Gaussian prior based on circular harmonic expansion," in *Proc. Hands-free Speech Comm. Microphone Arrays (HSCMA)*, San Francisco, Mar. 2017, pp. 196–200.